



Neuronal GPR81 regulates developmental brain angiogenesis and promotes brain recovery after a hypoxic ischemic insult

Prabhas Chaudhari^{1,2}, Ankush Madaan^{1,3}, José Carlos Rivera^{1,4,5} , Iness Charfi^{2,3}, Tiffany Habelrih¹ , Xin Hou¹, Mohammad Nezhady¹, Gregory Lodygensky¹, Graciela Pineyro^{1,2,3}, Thierry Muanza² and Sylvain Chemtob^{1,3,4,5}

Abstract

Perinatal hypoxic/ischemic (HI) brain injury is a major clinical problem with devastating neurodevelopmental outcomes in neonates. During HI brain injury, dysregulated factor production contributes to microvascular impairment. Glycolysis-derived lactate accumulated during ischemia has been proposed to protect against ischemic injury, but its mechanism of action is poorly understood. Herein, we hypothesize that lactate via its G-protein coupled receptor (GPR81) controls postnatal brain angiogenesis and plays a protective role after HI injury. We show that GPR81 is predominantly expressed in neurons of the cerebral cortex and hippocampus. GPR81-null mice displayed a delay in cerebral microvascular development linked to reduced levels of various major angiogenic factors and augmented expression of anti-angiogenic Thrombospondin-1 (TSP-1) in comparison to their WT littermates. Coherently, lactate stimulation induced an increase in growth factors (VEGF, Ang1 and 2, PDGF) and reduced TSP-1 expression in neurons, which contributed to accelerating angiogenesis. HI injury in GPR81-null animals curtailed vascular density and consequently increased infarct size compared to changes seen in WT mice; conversely intracerebroventricular lactate injection increased vascular density and diminished infarct size in WT but not in GPR81-null mice. Collectively, we show that lactate acting via GPR81 participates in developmental brain angiogenesis, and attenuates HI injury by restoring compromised microvasculature.

Keywords

Neonatal hypoxia-ischemia, GPR81, lactate, neurons, TSP-1, VEGF, brain microvasculature

Received 18 August 2021; Revised 9 November 2021; Accepted 10 December 2021

Introduction

Hypoxia-ischemic encephalopathy (HIE) in the neonate is a major cause of neurodevelopmental injury, which predisposes to neuropsychological disorders like epilepsy, mental retardation, cerebral palsy and learning disabilities.^{1,2} It is estimated that 4 in 1000 births are susceptible to HIE.³ Current health care focuses in understanding the pathophysiology of HIE in order to develop effective interventions for newborns at risk of cerebral hypoxic ischemia.^{1–3} In this context cerebral (hypoxic-ischemic) HI event triggers various adverse processes including glutamate toxicity,

¹Departments of Pediatrics, Ophthalmology and Pharmacology, CHU Sainte-Justine Research Center, Montréal, Canada

²Department of Experimental Medicine, McGill University, Montréal, Canada

³Department of Pharmacology, McGill University, Montréal, Canada

⁴Department of Ophthalmology, Université de Montréal, Montréal, Canada

⁵Maisonneuve-Rosemont Hospital, Research Center, Montréal, Canada

Corresponding authors:

Sylvain Chemtob, CHU Sainte-Justine, Research Center, Departments of Pediatrics, Ophthalmology and Pharmacology, 3175 Chemin Côte Ste-Catherine, Montréal, Québec, Canada, H3T 1C5.
Email: sylvain.chemtob@umontreal.ca

José Carlos Rivera, CHU Sainte-Justine, Research Center, Departments of Pediatrics, Ophthalmology and Pharmacology, 3175 Chemin Côte Ste-Catherine, Montréal, Québec, Canada, H3T 1C5.
Email: jc.rivera@umontreal.ca

generation of superoxide radicals, apoptosis, inflammation resulting in neuronal cell death,^{3,4} and associated with an underlying microvascular degeneration which contributes significantly to the brain injury.⁴

Recent research in regenerative biology has shed insights on brain's innate ability to limit damage during a recovery phase following HI insult.⁴ The recovery phase is characterized by neurorestorative changes in neurogenesis, synaptic remodeling and angiogenesis, which possess potential advantages over conventional neuroprotective therapies.⁵⁻⁷ Promoting angiogenesis immediately after HIE could potentially support tissue regeneration and neuron survival particularly as it pertains to the penumbra of the infarcted brain region. However, molecular triggers of angiogenesis need to be better elucidated in order to develop novel therapeutics for HIE.⁷⁻⁹ In this context, active neurons utilize glucose and oxygen to stay metabolically and functionally active.¹⁰ But insufficient supply of O₂ and nutrients causes neuronal distress and an aberrant cascade of mechanisms that partake in cerebrovascular injury.¹¹⁻¹³ Hence not surprisingly, disruption of brain metabolism is a key element in HIE. For instance, early phase of HIE is characterized by an arrest in oxidative phosphorylation resulting in acute accumulation of carbohydrate metabolites such as succinate, α -ketoglutarate and especially lactate.¹⁴⁻¹⁶ However, nature has adapted itself such that these ligands are not only intermediates of metabolism but also coordinate physiological and cellular processes by acting as recently shown through cognate G-protein coupled receptors (GPCRs).^{5,6} Succinate was identified as the ligand for GPR91 present in the cerebral cortex and implicated in revascularization after hypoxic-ischemia.¹⁷ α -ketoglutarate, the ligand for GPR99 is located in retinal ganglion cell neurons and is known to play an important role in axon growth.¹⁵ For its part, lactate exerts its biological effects via GPR81, also known as hydroxycarboxylic acid receptor (HCA1 or HCAR1).^{18,19} GPR81 has been implicated in several functions including attenuation of inflammation^{19,20} and regulation of angiogenesis in the developing retina as recently reported by us²¹ and cancer.^{18,19} GPR81 is expressed in several tissues including brain, where its activation has been associated with neuronal activity and energy metabolism.²² Others have proposed that neuronal progenitors are strictly dependent on lactate metabolism;²³ exogenous lactate supplementation immediately increases cerebral blood flow upon cerebral ischemic insult.²⁴ Conversely, some studies have proposed that lactate receptor antagonism can protect against ischemic brain injury;²⁵ however, there is uncertainty as to the interpretation of these pharmacological results using the non-selective ligand 3-hydroxybutyrate, which primarily stimulates

a different receptor, specifically HCAR2.²⁶ Hence, the role of GPR81 and its ligand lactate during brain development and ischemic brain injury, and mechanisms implicated remain unclear. In this study, we seek to elucidate the involvement and mechanism by which GPR81 can affect cerebral hypoxia-induced brain damage in a post-natal model of hypoxic-ischemic injury in mice. Our findings reveal new evidence that GPR81 contributes to brain vascular development and protects against hypoxic-ischemic damage, at least partly through release of angiogenic factors and suppression of anti-angiogenic ones.

Material and methods

Animals

C57BL/6 mice were obtained from The Jackson Laboratory. Adoptive lactating CD-1 females were purchased from Charles River Inc. (Montreal, CA) to tend to C57BL/6J pups. GPR81^{-/-} mice were obtained from Lexicon Pharmaceuticals (Texas, USA). The GPR81^{-/-} mice were backcrossed with adult C57BL/6 mice (The Jackson Laboratory) to obtain a pure C57/BL, as described by us.^{21,27} The transmembrane domain 2 of murine GPR81 coding region (100 base pairs) is replaced by a 4-kb IRES-lacZ-neo cassette. Mice were maintained on standard laboratory chow under a 12:12 light:dark cycle and allowed free access to chow and water. All experimental protocols were approved by the Animal Care Committee of Sainte-Justine's Hospital and conducted in accordance with guidelines established by the Canadian Council on Animal Care and the Animal Research Reporting *In Vivo* Experiments (ARRIVE) guidelines.²⁸

Immunohistochemistry

GPR81 protein localization was performed on 12 μ m coronal or sagittal sections of brain tissues or in primary neurons cultures fixed with 4% paraformaldehyde. The brains were then adequately dehydrated in sucrose 30% solution for 48 to 72 h at 4 °C. Brain sections or slides with neurons were then blocked with 5% bovine serum albumin and 0.1% TritonX-100 (T-8787; Sigma) in PBS and were subsequently incubated overnight with rabbit anti-GPR81 (Sigma; 1/500), mouse anti-NeuN (Millipore; 1/100), mouse anti-GFAP (IF03L-100 μ g (Millipore), 1/100) mouse anti-TSP-1 (Abcam 1:200) or anti-VEGF (Santa Cruz 1:200). Secondary antibodies conjugated with Alexa Fluor (Molecular Probes) directed against mouse (1:1000; Alexa Fluor 488, #A11070) and rabbit (1:1000; Alexa Fluor 594, #A11012) were incubated for 2 hours at

room temperature. Nuclei were stained with DAPI (Invitrogen; 1/1000); notably, tissues from GPR81-null mice did not display immunoreactivity to GPR81 antibody (Suppl Fig. 1A). Images were captured using 20x and 40x objective with Eclipse E800 (Nikon) fluorescence microscope.

Lectin staining

Brain tissue samples were collected after perfusion fixation with 4% paraformaldehyde as previously described.²⁹ Briefly, following anesthesia with 3% isoflurane, the animals were cut open below the diaphragm and the rib cage was cut rostrally on the lateral edges to expose the heart. A small hole was cut in the left ventricle and the needle was inserted into the aorta and clamped, then the right atrium was cut to allow flow. The animals were transcardially perfused with PBS for 4–5 minutes or until liver was cleared of blood. Next, we perfuse mice with 4% paraformaldehyde for 4 minutes. Then, entire brain was dissected and further immerse in 4% paraformaldehyde for 24 h at 4 °C. Tissue was then transferred to 30% sucrose solution overnight and then cut. Vessels density was evaluated on 12 μm brain cryosections stained with *Griffonia simplicifolia* (1:100, Sigma). The vessel density

in the cortical area was calculated by averaging 4–5 consecutive (20X magnification) sections from 5 animal brains per group using image J software (NIH software) as previously reported.^{6,17} The density of the vessels in the cortical area of GPR81KO mice was comparable to the cortical area in control animals injected with vehicle (PBS). Vessel density was expressed as the percentage total area covered by lectin staining.

Primary neuronal cell culture

C57BL/6 pups (P0-P3) were decapitated following cryoanesthesia, then their brains were rapidly removed and transferred into ice-cold dissociation solution (Na₂SO₄ 90 signaling; K₂SO₄30 signaling; MgCl₂ 5.8 signaling; CaCl₂; HEPES 10 signaling; glucose 20 mM; pH 7.4). The brain was then cut into two halves by at the mid hemisphere. The meninges were carefully removed, and the cerebellum was discarded. Under the dissecting microscope the midbrain and thalamus were carefully removed until the horseshoe structure of hippocampus was seen. By using a pair of forceps, the meninges surrounding the hippocampus was removed and discarded. The isolated hippocampi were transferred to dissociation medium and washed twice each with 10 ml volume. Hippocampi isolated

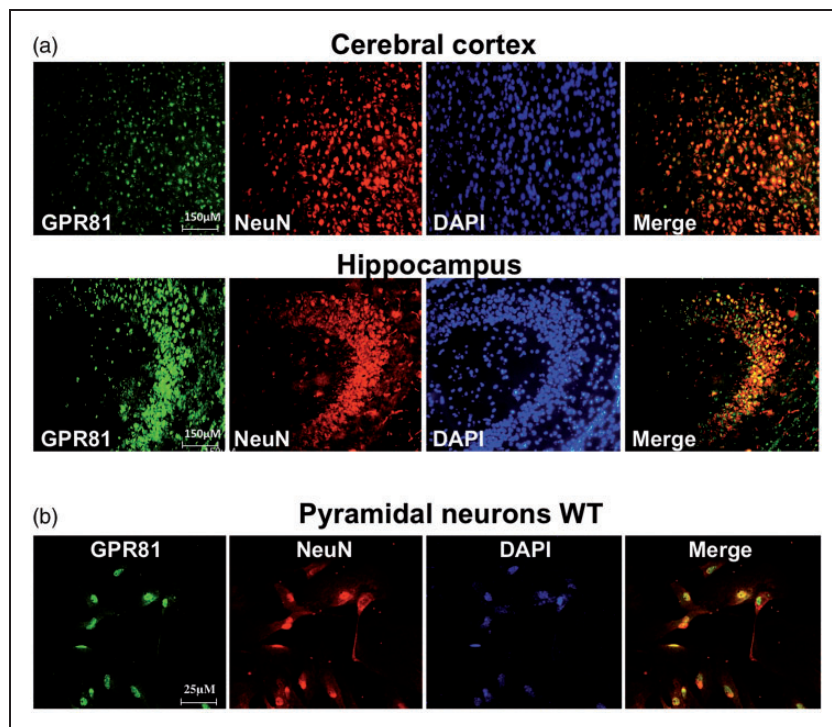


Figure 1. Lactate receptor GPR81 localization in mouse brain. (a) Representative confocal images of brain sections showing colocalization of GPR81 (green) with the specific neuronal marker NeuN (red) in cerebral cortex and hippocampus. Nuclei were counterstained with 4',6-diamidino-2-phenylindole (DAPI) and merged images (yellow) show the colocalization. Scale bar, 150 μm. (b) Immunoreactivity to GPR81 (green) was also present in NeuN+ (red) pyramidal hippocampal primary cell. Nuclei were counterstained with 4',6-diamidino-2-phenylindole (DAPI) and merged images (yellow) show co-localization. Scale bar, 25 μm.

from the brain was minced and rinsed in HBS solution under sterile condition. Minced tissues were treated with trypsin and were incubated for 20 mins at 37°C. Cells were then separated by trituration using polished pipettes. The dispersed cells were then plated on polylysine-coated slides in petri dishes. After plating, cells were incubated at 37°C in 5% CO₂ and incubated for 2 to 5 days. After which the cells were subjected to immunohistochemistry analysis or western blotting.

Hypoxic treatment of neurons

Primary neurons were cultured on poly-lysine coated 12 well plates in an external hypoxic chamber (5% O₂ [5% CO₂, 37°C]) for 24 hours³⁰ in presence or absence of lactate. PBS and lactate-conditioned media was collected after this time and used to determine the production of angiogenic factors, or to evaluate angiogenic response in *ex-vivo* aortic explants after 96 hours of incubation with the media.

Real time PCR

Brain tissues were snapped freeze in solid CO₂ and mRNA was isolated from the cerebrum as per the manufactures protocol. The RNA concentration and integrity were measured with a NanoDrop 1000 spectrophotometer. Reverse transcription was carried out using MMLV kit protocol from life technologies or cDNA synthesized using iScript cDNA SuperMix (Biorad laboratories). Primers were obtained from alpha DNA, forward primer (sequence) and reverse primer (sequence). Quantitative gene expression analysis was performed on Stratagene MXPro3000 (Stratagene) with SYBR Green Master Mix (BioRad). Expression was normalized to 18S universal primer (Ambion) and calculation made using the Ct method. The PCR reaction was carried out at 95°C-5 mins, 95°C-30 sec, 58°C-30 sec, and 72°C-30 sec. Dissociation curves were also acquired to test primer specificity.

Western blotting

Proteins from homogenized brains were lysed in RIPA buffer and quantified using Bradford's method (Bio-Rad). 50 µg of protein sample was loaded onto SDS-PAGE gel and electrotransferred onto PVDF membranes. Aged match tissue samples (P7, P9 and P11) and neurons from WT and GPR81-null mice were plated up to 400,000 cells per well in 12 well plate and incubated overnight in Neurobasal media with B27 supplement. Cells were treated with PBS or lactate (10 mM) for 24h, and the ligand binding reaction was inhibited by addition of 2 ml ice-cold PBS.

300 µl of ice-cold RIPA buffer was added to lyse the cells. The cells were scraped off and agitated on a rocking platform for 1 h at 4°C. The lysate was further centrifuged for 30 mins at 13000xg at 4°C. The supernatant was electrophoresed on 15% polyacrylamide gel for 2 h, after which it was transferred to a PVDF membrane. The membranes were immunoblotted using anti-GPR81 (SAB1300790, Sigma-Aldrich) antibody (1:250), anti-TSP-1 (Abcam, 1:200), anti VEGFA (Santa cruz 1:200) and were detected with their respective secondary antibodies conjugated to HRP substrate. Enhanced chemiluminescence (GE Healthcare) was used for detection using the ImageQuant LAS- 500 (GE Healthcare, Little Chalfont, United Kingdom). Relevant herein, GPR81 immunoreactivity was absent in tissues of GPR81-null mice (Suppl Fig. 1).

Aortic explants

Aortas were extracted from adult C57BL/6 mice, cut into 1 mm rings, and placed in growth factor reduced Matrigel (BD Biosciences) in 24-well tissue culture plates as previously reported.⁶ The explants were cultured for 5 days in media conditioned by primary neurons from WT and GPR81^{-/-} mice previously exposed to normoxia (21% O₂) or hypoxia (5% O₂). Neutralizing antibodies against TSP-1 (1.2 µg/ml; EMD Millipore) were used in some cases. Microvascular sprouting of the individual explants was quantified by measuring the area covered by outgrowth of the aortic ring with image J software (NIH software) as reported.³¹ Briefly, the images were analyzed for total outgrowth using color-based threshold to record only microvascular outgrowth and not the aortic segment. Vascular outgrowth was measured as the percent of the total image area occupied by vascular structures.

Animal experimentation and Rice-Vannucci model

Cerebral hypoxia-ischemia was generated on C57BL/6 wild-type and GPR81^{-/-} mice using the Rice-Vannucci model. Briefly, 7-day-old (P7) mice were anesthetized in 3% isoflurane in oxygen and subject to permanent unilateral ligation of the common carotid artery, followed by exposure to 7% O₂ for 120 min at 37°C.³² Intracerebroventricular injections of lactate were performed on pup mice at P4 as previously reported.¹⁷ Briefly, pup mice were anesthetized with 3% isoflurane. Then, a 10 µL Hamilton syringe (Hamilton, Reno, NV) was used to inject 2 µL of 100 mM lactate [estimated brain volume 0.1 ml]^{17,33} or PBS (for control animals) into the right cerebral ventricle (stereotaxic coordinates: PA-1.0 mm,

lateral-1.0 mm from bregma and ventral -2.0 mm relative to dura).

Infarct volume

Infarct volumes were measured using 2,3,5-Triphenyltetrazolium chloride (TTC) staining as described.^{34,35} The principle is based on mitochondrial damage, lesser insult results in faint pink staining called the penumbra, and normal cells show bright reddish-pink staining indicating normal active metabolic tissue. This is a semi-quantitative method used for determining the infarct size. After 96 h of hypoxic-ischemic exposure of the pups the brains were rapidly removed and frozen in isopentane solution. The cryofrozen fresh tissue was stored at -20°C until further use. The whole brain was immersed in the solution for topical TTC staining to determine global infarct area. The slices and or whole brain were then quickly transferred to a 0.1% TTC solution prepared in PBS buffered at pH 7. The brains were then incubated at 37°C for 30 min away from light. The area of infarcted region on the ipsilateral side and the undamaged region on the contralateral side were measured using ImageJ.³⁶

Statistical analysis

All data were analyzed using GraphPad Prism software version 6.0 (GraphPad Software, San Diego, CA). Only mice that survived the full Rice-Vannucci model protocol were included in the experiments. Normality was assessed by the Shapiro-Wilk test. Two variants were compared by t-test (two-tailed) for independent samples for results of GPR81 WT vs KO comparison. Comparisons between several groups were performed using ordinary one-way ANOVA; Dunnett's multiple comparison method was used as a post-hoc test when treatments were compared with one control. Descriptive statistics, including means SD, have been reported. $P < 0.05$ was considered statistically significant.

Results

GPR81 receptor is prominently localized in neurons of the developing brain

We evaluated the localization of GPR81 receptor by dual immunohistochemical labeling using an anti-GPR81 antibody and specific cell markers against endothelial cells (Lectin+), astrocytes (GFAP+), mononuclear phagocytes (microglia [Iba-1]) and neurons (NeuN+) on coronal sections of brain tissue; GPR81 immunoreactivity is absent in GPR81KO

animals (Suppl. Fig. 1). GPR81 expression predominated in neurons (NeuN+ cells) of cerebral cortex and hippocampus (Figure 1(a)); GPR81 did not colocalize with endothelial cells, astrocytes and microglia (Suppl. Fig. 1). Presence of GPR81 in neurons was validated in cultured primary neonatal pyramidal neuronal cells isolated from the hippocampus of WT GPR81 (Figure 1(b)); as expected, brain homogenates from GPR81-null mice were devoid of GPR81 (Figure 2(a) and Suppl. Fig. 1D).

GPR81 participates in developmental brain angiogenesis by controlling angiogenic factors

GPR81 mRNA and protein expression increased gradually from P5 to P9 at which time it reached a peak (Figure 2(a) and (b)). Based on previous findings that GPR81 regulates deep neuro-retinal vascular development,²¹ we predicted that GPR81 may have a similar role in postnatal brain vascular development. Brain microvasculature evaluated by confocal microscopy revealed a developmental delay in GPR81-null mice compared to WT animals prior to P15 (Figure 3); thereafter, possible compensatory mechanisms participate in catch-up development.^{37,38}

GPR81 and other receptors for metabolic intermediates such as GPR91 (succinate receptor) are reported to control angiogenic processes.^{17,21,33,39} We evaluated the expression of select major angiogenic and inflammatory factors (known to affect angiogenesis) in the developing brain (Figure 4 and Suppl. Fig. 2) of WT mice, notably VEGF-A, Ang-1, Ang-2, PDGFBB, CCL2, COX-2 and anti-angiogenic TSP-1. All angiogenic factors measured increased during early post-natal life and peaked by P9 (Figure 4), akin to GPR81; while TSP-1 expression displayed a decreased expression during the same period; CCL2 and COX-2 had a modest <2-fold decrease over the same age span (Suppl Fig. 2). GPR81 gene knock out reversed changes in all factors measured over the same age period, including increases in TSP-1 and in pro-inflammatory COX-2 and CCL-2 (Fig. 4; Suppl Fig. 2). By P15 the expression levels of all factors normalized in GPR81-null mice coinciding with catch-up of brain microvascular density (Figures 3 and 4 and Suppl. Fig. 2). These observations suggest that GPR81 regulates key factors associated with the control of the cerebral microvascular development during early postnatal ontogeny.

Based on presence of GPR81 in neurons we surmised that lactate stimulation of these cells would induce generation of major angiogenic factors; indeed, lactate stimulation of GPR81 in isolated neurons increased VEGF-A expression and conversely decreased the expression the anti-angiogenic factor

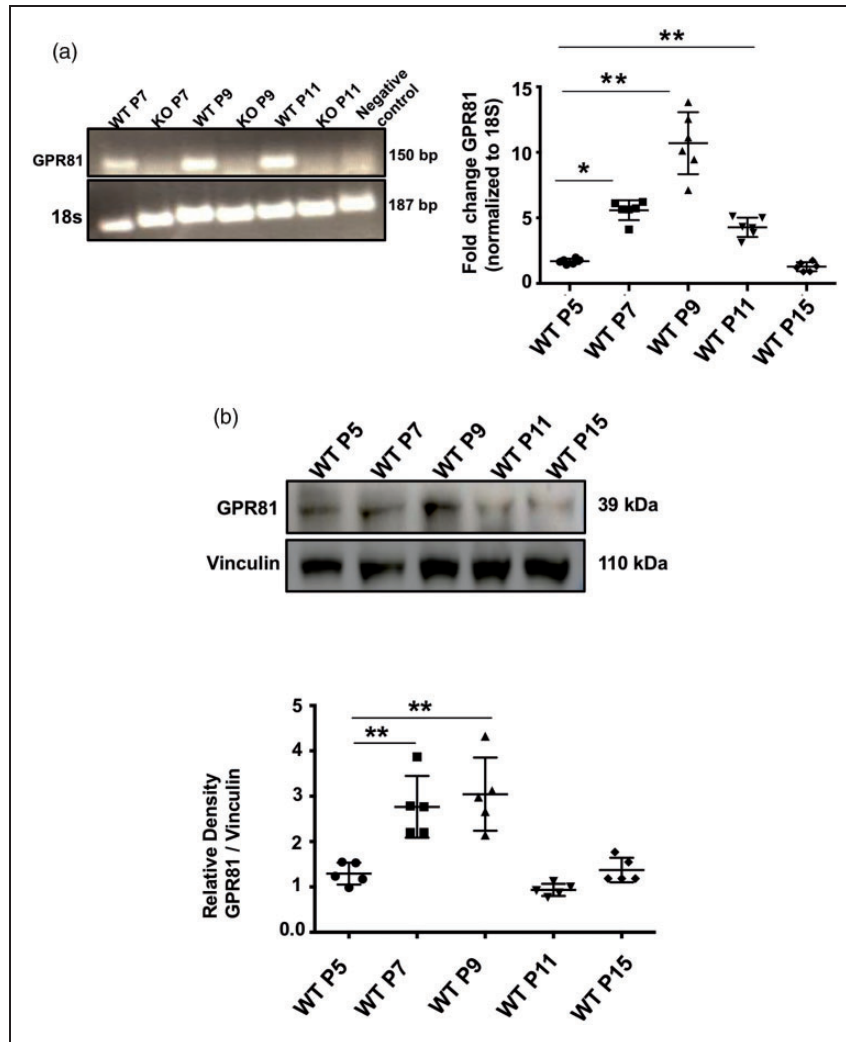


Figure 2. GPR81 levels during developmental cerebral angiogenesis. (a) GPR81 expression (150 bp) evaluated by reverse-transcriptase-PCR was detected in brain homogenates from WT mice, but it was absent in brain samples from GPR81-null mice; 18S (187 bp) was used as an internal control. Real-time quantitative PCR was used to determine ontogenic expression of GPR81 at different postnatal (P) ages (P5, P7, P9, P11 and P15). Data represent mean \pm SD; $n = 6$ animals per group; * $p < 0.05$, ** $p < 0.01$ compared to P5, one-way ANOVA followed by the Dunnett's test for multiple comparison with control. (b) Western blot analysis of GPR81 (39 kDa) expression levels in brain samples from WT mice at different postnatal ages (P5, P7, P9, P11 and P15). Vinculin (110 kDa) was used as internal controls. Data represent mean \pm SD; $n = 5$ animals per group. ** $p < 0.01$ compared to P5; one-way ANOVA followed by the Dunnett's test for multiple comparison with control.

TSP-1 (Figure 5(a); Suppl Fig. 3). Correspondingly, conditioned media of lactate-stimulated isolated neurons induced microvessel sprouting of aortic explants in Matrigel (Figure 5(b)); neurons devoid of GPR81 did not respond to lactate.

Consistent with *ex vivo* observations (Figure 5(b)) intra-cerebroventricular injections of lactate *in vivo* at P4 accelerated brain vascularization (measured at P5) in WT but not in GPR81-null subjects (Figure 6(a)). Coherently, lactate augmented levels of proangiogenic VEGF-A, Ang-1, Ang-2, PDGF, and suppressed that of angiostatic factor TSP-1 (Figure 6(b)) in WT

animals (Figure 6(b)); lactate was ineffective in GPR81-null mice.

Lactate reduces infarct size secondary to perinatal HI insult

To further explore the role of GPR81 we investigated its involvement in brain hypoxia-ischemic (HI) insult. Newborn mice (P7) were subjected to permanent left carotid artery ligation followed by hypoxic (8% O_2) exposure for 1.5 hours as documented;^{6,17} lactate (estimated intra/periventricular concentration: 10 mM) was

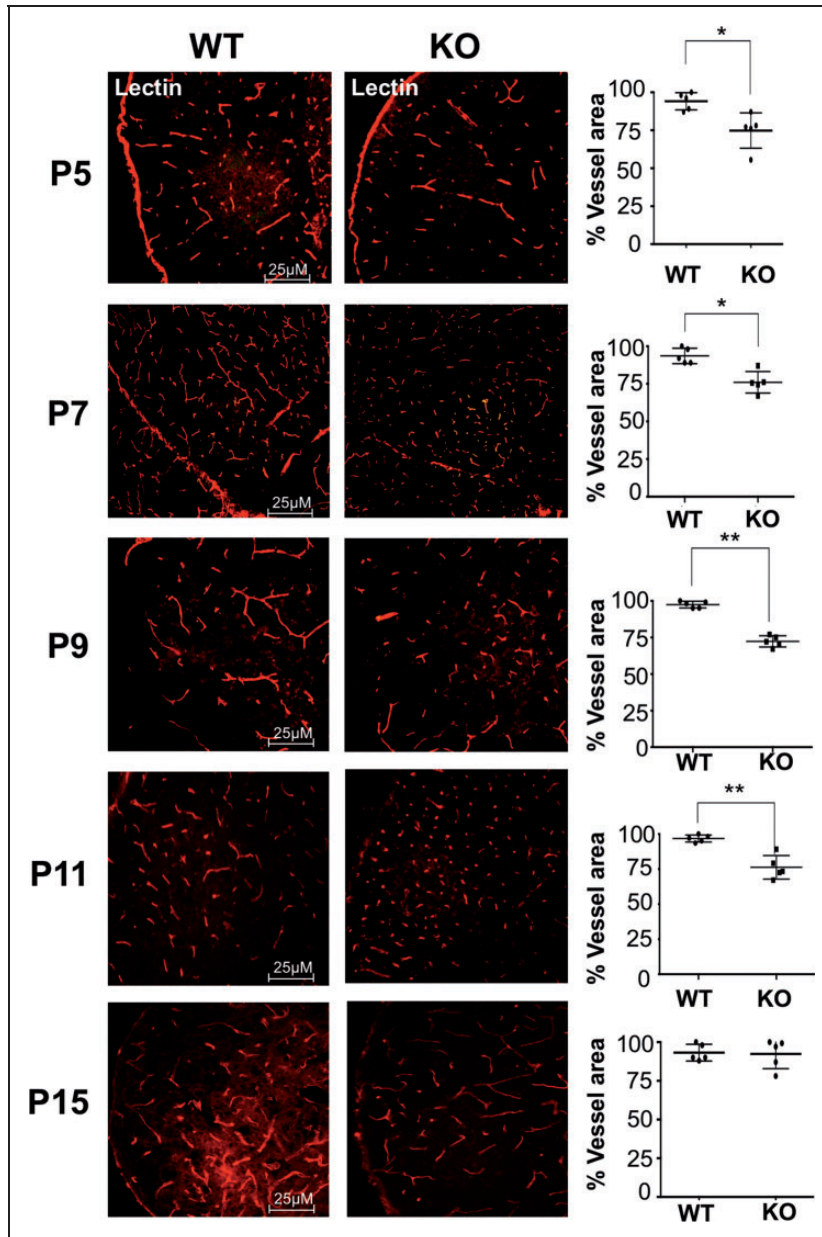


Figure 3. Brain vascular development is delayed in GPR81-null mice. Representative confocal images of brain slices stained with lectin, showing brain vasculature in the cortex from age-matched GPR81-null and WT mice collected at different post-natal days (P5, P7, P9, P11 and P15). Histograms represent the percentage of vascular area in the cortex from WT versus GPR81-null mice. Values represent mean \pm SD; $n = 5$ animals per group; * $p < 0.05$, ** $p < 0.01$ compared with corresponding WT, Student's t-test.

injected at P4. Lactate reduced infarct size by $\sim 50\%$ 96 h post-HI in WT mice; conversely, infarct size was increased in GPR81-null mice, where lactate was ineffective (Figure 7(a)). Consistently, vascular density in the peri-infarct area (penumbra) was augmented by lactate in WT mice and diminished in GPR81-null mice at 48 and 96 h post-HI. (Figure 7(b)). Lactate-induced angiogenesis was associated with a coherent increase in pro-angiogenic factors (VEGF-A, PDGF-BB, Ang-1 and Ang-2) and suppression of anti-angiogenic TSP-1

in WT animals (Figure 7(c)); lactate was ineffective in GPR81-null mice.

Angiogenic effects of hypoxic neurons were corroborated *in vitro* by exposing to hypoxia (5% O₂) primary neurons from WT and GPR81-null mice. After 24 h the conditioned media was collected and used in aortic explants to evaluate the pro-angiogenic activity. Vascular sprouting was increased by lactate-treated neurons and abolished in conditioned media from neurons of GPR81-null mice (Suppl Fig. 4A), in line with

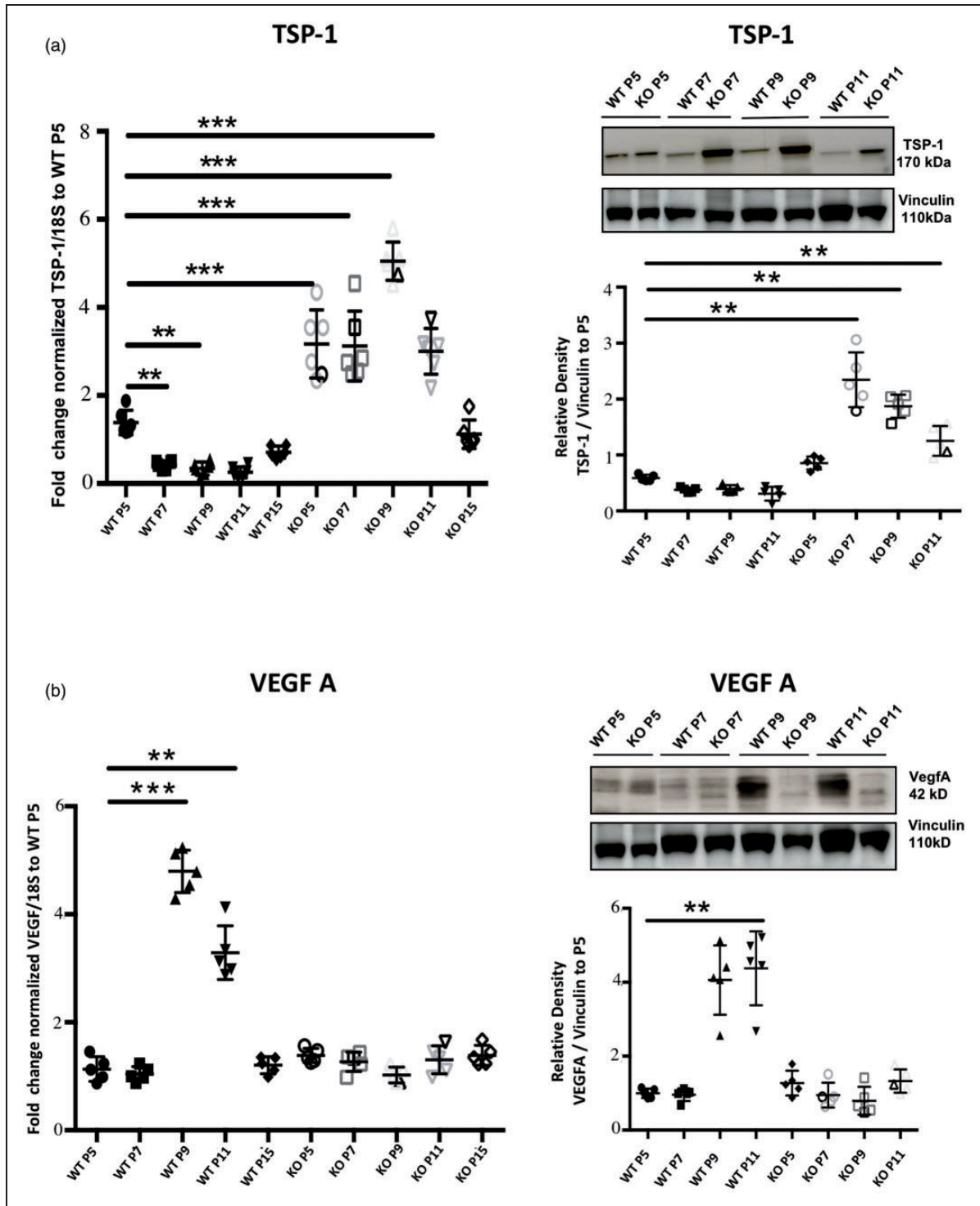


Figure 4. Delayed vascular development in GPR81-null mice brain is associated with a decreased VEGF expression and increased levels of the antiangiogenic TSP-I factor. Real-time quantitative PCR and Western blot analysis of (a) TSP-I (170 kDa) and (b) VEGF-A (42 kDa) expression levels in brain samples from WT and GPR81-null mice at different postnatal (P) ages. 18S and Vinculin (110 kDa) were used as internal controls for qPCR and Western blot respectively. Data represent mean \pm SD; n = 5 animals per group; **p < 0.01, ***p < 0.001 compared to WT P5; one-way ANOVA followed by the Dunnett's test for multiple comparison with control.

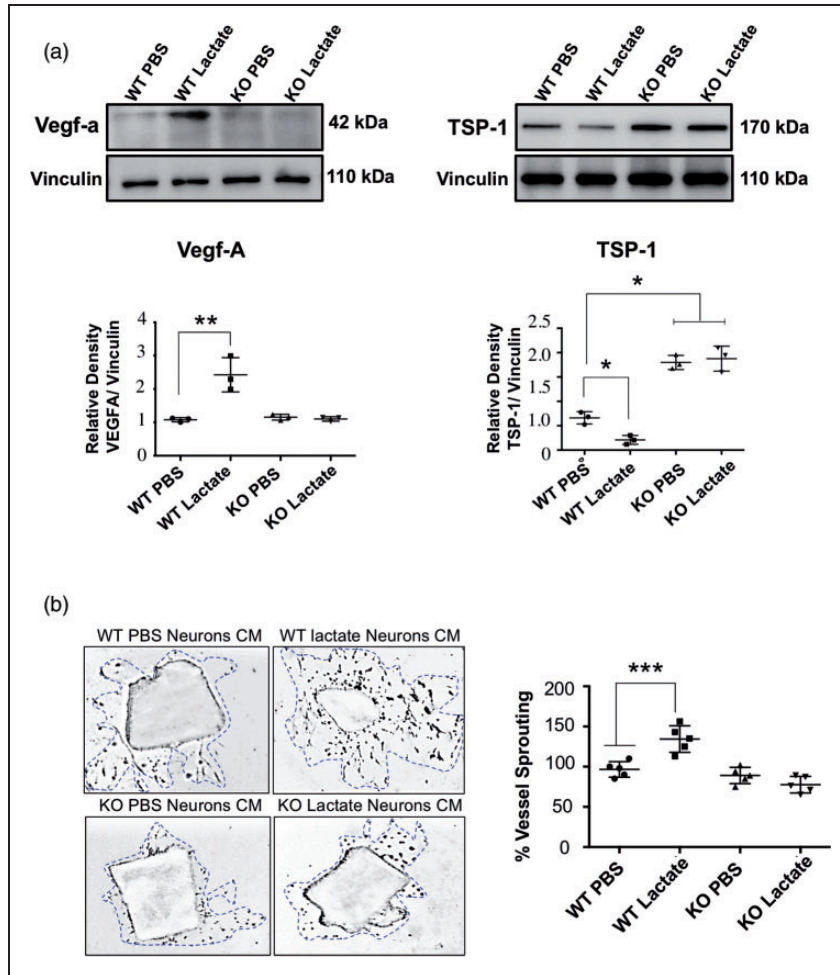


Figure 5. Proangiogenic effects of lactate are GPR81-dependent. (a) Western blot analysis of VEGF (42 kDa) and TSP-1 (170 kDa) protein levels in cell lysates from WT- and GPR81-null mice-derived neurons previously stimulated with lactate (10 mmol/L) or vehicle (PBS). Vinculin (110 kDa) was used as internal controls. Densitometry quantification is illustrated in the histogram. Data are expressed as mean \pm SD; $n = 3$ experiments per group; * $p < 0.05$, ** $p < 0.01$ compared to corresponding WT PBS neurons, one-way ANOVA followed by the Dunnett's test for multiple comparison with control. (b) Representative microvascular sprouting of Matrigel-embedded aortic explants treated with conditioned media from WT- and GPR81-null mice-derived neurons previously stimulated with lactate (10 mmol/L) or vehicle (PBS) after 48 hours. Histogram represent the quantification of the aortic vessel sprouting (blue dotted lines). Values represent mean \pm SD; $n = 5$ aortic explants per group. *** $p < 0.001$ compared to WT PBS neurons, one-way ANOVA followed by the Dunnett's test for multiple comparison with control.

coherent changes in VEGF-A and TSP-1 (Suppl Fig. 4B). Role of TSP-1 was established using a neutralizing antibody in the conditioned media from GPR81-KO neurons (treated with lactate); anti-TSP-1 antibody restored angiogenic sprouting in aortic explants (Suppl Fig. 4A).

Discussion

A number of major angiogenic factors such as VEGF, PDGF, Ang-1/2, FGF contribute to fetal/neonatal brain vascular development.⁴⁰ Yet, the most prominent physiologic process that triggers brain vascular development is hypoxia.^{11,41,42} Relevantly, similar

mechanisms also contribute to angiogenesis following HIE where recovery after a HI insult is attributed to an intricately organized process of neovascularization.^{36,43} In both ontogenic and pathogenic conditions angiogenesis restores blood perfusion to reinstate adequate O_2 and nutrient supply.⁴⁴ In addition to well established hypoxia-triggered HIF-1 α and adenosine formation which exhibit relatively short durations of action (hours vs days of development),⁴⁵ other mechanisms are likely to participate in this more prolonged process.⁴⁶ In this context, lactate is well known to accumulate during hypoxia. For long this metabolite was simply thought to be an inert intermediate of metabolism. Later, lactate was found to exhibit a number of

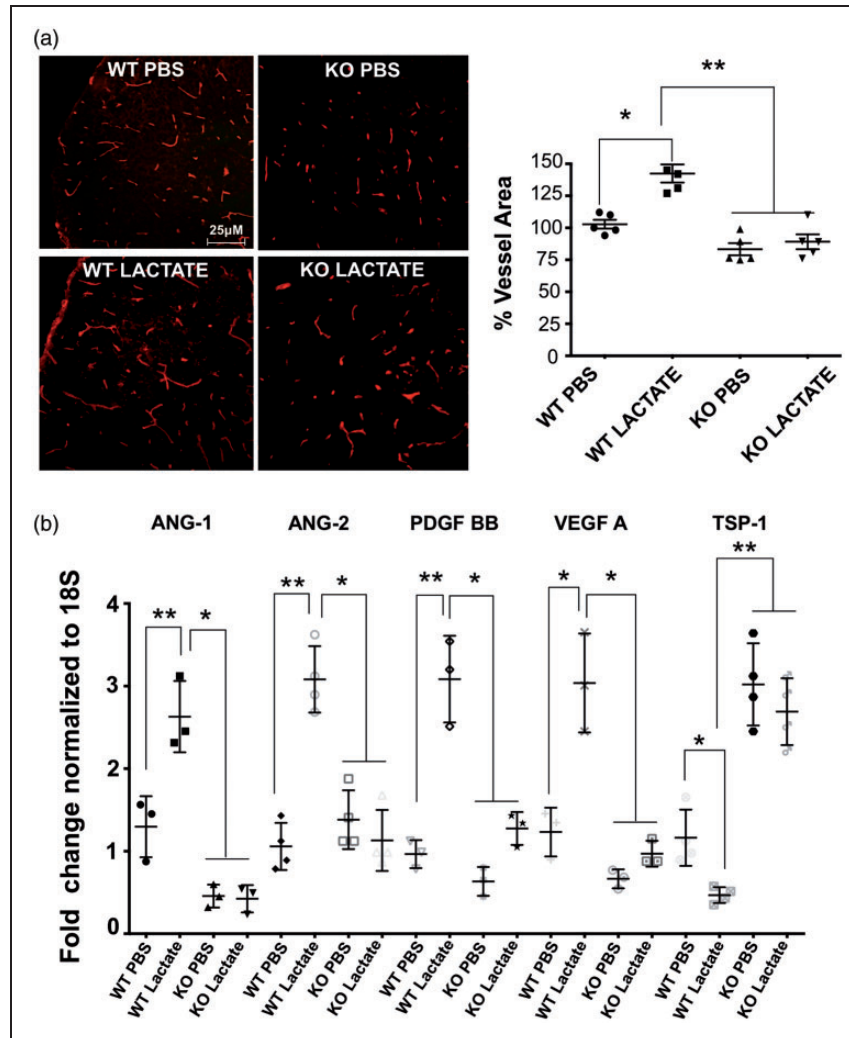


Figure 6. Lactate acting via GPR81 augments brain vascular density by increasing VEGF expression and suppressing TSP-1. (a) Representative confocal images of lectin-stained (red) brain cross-sections (in P5) showing a marked (25%) increase in cerebral vasculature in the cortex from WT mice compared to age matched GPR81-null mice, 24 hours after intra-cerebroventricular lactate injections. Histogram represent the quantification of the brain vascular area in the cortex area from WT versus KO GPR81-null mice at P5. Values represent mean \pm SD; $n = 5$ animals per group. * $p < 0.05$, ** $p < 0.01$ compared to WT PBS, one-way ANOVA followed by the Dunnett's test for multiple comparison with control. (b) Real-time quantitative PCR analysis showing the mRNA expression of proangiogenic factors VEGF, ANG-2, PDGF; anti-angiogenic factor TSP-1 and pro-inflammatory factors COX-2 and CCL-2 in WT mice and GPR81-null mice, 24 hours after intra-cerebroventricular lactate injections. Values represent mean \pm SD; $n = 4-5$ samples per group. * $p < 0.05$, ** $p < 0.01$ compared to their respective control; one-way ANOVA followed by the Dunnett's test for multiple comparison with control.

properties such as synaptic plasticity⁴⁷ neuroprotection,⁴⁸ suppression of inflammation,⁴⁹ and induction of angiogenesis.^{50,51} Interestingly, as observed for other receptors of intermediate metabolism⁵² a receptor for lactate was identified, specifically GPR81,⁵³ which transduces signals for more sustained effects. Consistent with high extracellular concentrations of lactate, GPR81 displays affinity in the millimolar range.⁵⁴ Other than in adipocytes where originally detected,⁵⁵ GPR81 is also found in endothelium,

macroglia, and mononuclear phagocytes.⁵⁴ Given that GPR81 is a receptor for a hypoxia-accumulated ligand namely lactate, that developmental expression in GPR81 can affect vascular development,²¹ and that basal GPCR activity can exist independent of ligand activation,⁵⁶ we surmised that GPR81 is a worthy candidate to contribute to ontogenic brain vascular development as well as that elicited during HI insult. We hereby show that the metabolic sensing receptor GPR81 is predominantly expressed in brain neurons,

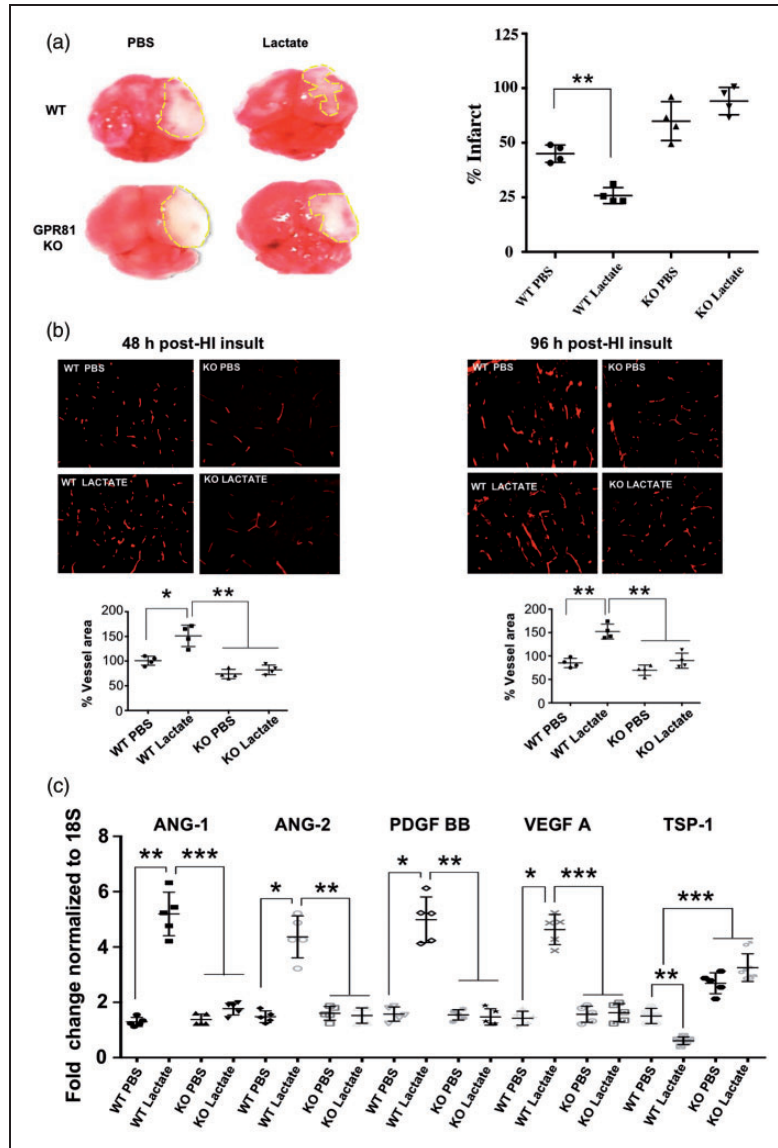


Figure 7. Lactate reduces infarct size and concordantly augments cerebral vascular density following perinatal HI insult.

(a) Tetrazolium chloride (TTC) staining in brains showing infarct size (dotted lines) in WT compared to GPR81-null mice after intra-cerebroventricular lactate (10 mmol/L) injections. Histograms represent infarct size (percentage) in WT versus GPR81-null mice. Values represent mean \pm SD; $n = 4$ animals per group. ** $p < 0.01$ compared to WT PBS; one-way ANOVA followed by the Dunnett's test for multiple comparison with control. (b) Representative confocal images of lectin-stained (red) brain cross-sections (in P5) showing vasculature mostly in the periinfarct area of cortex from WT mice and age matched GPR81-null mice pre-treated with lactate or PBS (vehicle) and evaluated after 48 hours and 96 hours post-HI. Histograms represent percentage of vessel area in WT versus GPR81-null mice after lactate treatment. Values represent mean \pm SD; $n = 4$ animals per group. * $p < 0.05$, ** $p < 0.01$ compared to WT PBS; one-way ANOVA followed by the Dunnett's test for multiple comparison with control. (c) Real-time quantitative PCR analysis showing the mRNA expression of proangiogenic factors VEGF, ANG-1, ANG-2, PDGF; anti-angiogenic factor TSP-1 in brain tissues from WT and GPR81-null mice, 48 hours after HI insult and intra-cerebroventricularly injected or not with lactate. Data represent mean \pm SD; $n = 5$ samples per group; * $p < 0.05$, ** $p < 0.01$, *** $p < 0.001$ compared with WT PBS, one-way ANOVA followed by the Dunnett's test for multiple comparison with control.

and plays a significant role in brain angiogenesis during development as well as in response to HI insult, by oppositely modulating the expression of pro- and anti-angiogenic factors (see schematic diagram in Suppl Fig. 5).

An important feature of this study applies to the mechanism by which GPR81 activation enhances angiogenesis and limits ischemic brain injury. GPR81 expression was found to increase during early postnatal brain development, particularly as it applies to

neurons. Lactate has been reported to exert neuroprotective effects.^{57,58} GPR81 was recently shown to rescue ischemic retinal tissue by inducing angiogenesis in an ischemic retinopathy model.²¹ We found that lactate increases brain vascular density and when administered prior to HIE in newborns it substantially diminishes infarct size; conversely lactate exposure in GPR81-null pups did not decrease infarct size, indicating that the protective effect of lactate is mediated by GPR81. Beneficial angiogenic effects of lactate acting via GPR81 were associated with an induction of various pro-angiogenic factors such as VEGF, ANG-2 and PDGFB and a significant decrease in TSP-1 as seen in isolated neurons, consistent with role of these factors on brain microvascular development.^{59,60} One cannot fully exclude that the effects of lactate could be ascribed to other functions mediated via the same^{49,50} or other cell types.^{61,62} Hence restoration of appropriate perfusion by inducing angiogenesis during stroke can ameliorate ischemia and improve outcome as previously suggested.⁶³ A similar paradigm had been proposed for the succinate receptor GPR91 in HIE; GPR91 promoted brain revascularization via a prostaglandin-mediated secretion of pro-angiogenic factors including VEGF, ANG-1, ANG-2 and IL-6.³⁹

TSP-1 is also an important endogenous inhibitor of angiogenesis. TSP-1 is produced and secreted by neurons and astrocytes in the brain, where it exerts an important role in neuronal and vascular development.⁶⁴⁻⁶⁷ However, its link to GPR81 has not been investigated. We found that TSP-1 expression is inversely associated to that of GPR81 during ontogeny and in response to HI insult, as observed during development, upon lactate stimulation, and by GPR81 gene knockout; this association between TSP-1 and GPR81 expression is reproduced *in vitro* on isolated neurons. TSP-1 exerts its effect by interacting with CD-36 and CD-47 receptors on endothelial cells, resulting in decreased proliferation via Akt and PI3K dependent signaling pathway;⁶⁸ TSP-1 also reduces VEGF-A⁶⁹ and nitric oxide mediated angiogenic response,⁷⁰ enhancing anti-angiogenic TSP-1 effects. Other than angiogenic factors, the pro-apoptotic anti-angiogenic TSP-1 can increase excitatory synapse formation via its interaction with brain voltage-dependent calcium channel $\alpha 2\delta 1$ receptor, leading to recurrent depolarizations and cytotoxicity;⁷¹ this effect is inhibited by gabapentin which interferes with interaction of TSP-1 with its $\alpha 2\delta 1$ receptor.⁷²

In addition to elevated TSP-1 levels in absence of GPR81, we also observed a corresponding increase in inflammatory factors CCL-2 and COX-2 in GPR81-null mice that could be detrimental to neurovascularization. This regulation of inflammatory

mediators by GPR81 is well documented by us and others.^{19,27} Collectively, GPR81 controls brain vascularization by governing expression of angiogenic and inflammatory factors.

GPR81 was largely localized in neurons, consistent with previous reports.⁶² Others have also identified it in vascular/perivascular brain cells.⁶³ We detected an increased expression of GPR81 during brain development from P7 to P11 in WT mice that normalized at P15 and coincided with vascular development as inferred to be by delay in vascular development in absence of GPR81, and conversely its acceleration upon lactate stimulation. This suggestion is consistent with a GPR81-dependent regulation of angiogenesis by modulating the expression of several growth factors as shown here and elsewhere.^{19,21,64}

Current treatments for HI stroke are based on therapies that involve rescue of neuronal insult via hypothermia, thrombolysis, and possible use of various growth factors and/or inhibitors of inflammation.⁷³ We have explored the role of the receptor for the metabolite lactate acting via GPR81 during development and post-HI brain vasculature, and have found it to be important in attenuating brain injury after HI stroke by enhancing revascularization via upregulation of angiogenic factors including VEGF-A and significantly down-regulating TSP-1. We surmise that selective long-acting GPR81 agonists may exert favorable outcomes in HI insults.⁵⁶

Funding

The author(s) disclosed receipt of the following financial support for the research, authorship, and/or publication of this article: This work was supported by Canadian Institutes of Health Research (CIHR) grant FRN12532 (S.C). P.C. was supported by a scholarship from the Suzanne Veronneau-Troutman Funds associated with the Department of Ophthalmology of Université de Montréal, by the Vision Research Network (RRSV), FRQS and CIHR. A.M. was recipient of the CIHR Drug Design Training Program (DDTP), Systems Biology Training Program (SBTP) and Vision Research Network (RRSV). S.C. holds a Canada Research Chair (Vision Science) and the Leopoldine Wolfe Chair in translational research in age-related macular degeneration.

Acknowledgments

We thank Lexicon Pharmaceuticals (Texas, USA) for the generous donation of the GPR81^{-/-} mice. All data generated in this study are included in this article.



Declaration of conflicting interests

The author(s) declared no potential conflicts of interest with respect to the research, authorship, and/or publication of this article.

Authors' contributions

PC, JCR and SC conceived and designed the experiments and wrote the manuscript. PC, AM, IC, TH, XH, and MN performed experiments. GL, GP and TM provided expertise advice. JCR designed and drew the scheme. All authors read and approved the final manuscript.

ORCID iDs

José Carlos Rivera  <https://orcid.org/0000-0003-2530-4433>
Tiffany Habelrih  <https://orcid.org/0000-0002-0923-9603>

Supplemental material

Supplemental material for this article is available online.

References

- Fatemi A, Wilson MA and Johnston MV. Hypoxic-ischemic encephalopathy in the term infant. *Clin Perinatol* 2009; 36: 835–858.
- Vannucci SJ and Hagberg H. Hypoxia-ischemia in the immature brain. *J Exp Biol* 2004; 207: 3149–3154.
- Gopagondanahalli KR, Li J, Fahey MC, et al. Preterm hypoxic-ischemic encephalopathy. *Front Pediatr* 2016; 4: 114.
- Nauta TD, van Hinsbergh VW and Koolwijk P. Hypoxic signaling during tissue repair and regenerative medicine. *Int J Mol Sci* 2014; 15: 19791–19815.
- Rana BK, Shiina T and Insel PA. Genetic variations and polymorphisms of G protein-coupled receptors: functional and therapeutic implications. *Annu Rev Pharmacol Toxicol* 2001; 41: 593–624.
- Honore JC, Kooli A, Hamel D, et al. Fatty acid receptor Gpr40 mediates neuromicrovascular degeneration induced by transarachidonic acids in rodents. *Arterioscler Thromb Vasc Biol* 2013; 33: 954–961.
- Thwaites JW, Reebye V, Mintz P, et al. Cellular replacement and regenerative medicine therapies in ischemic stroke. *Regen Med* 2012; 7: 387–395.
- Gonzalez FF, Larphaveesarp A, McQuillen P, et al. Erythropoietin increases neurogenesis and oligodendroglial cell precursor cells after neonatal stroke. *Stroke* 2013; 44: 753–758.
- Cao Y. Adipose tissue angiogenesis as a therapeutic target for obesity and metabolic diseases. *Nat Rev Drug Discov* 2010; 9: 107–115.
- Belanger M, Allaman I and Magistretti PJ. Brain energy metabolism: focus on astrocyte-neuron metabolic cooperation. *Cell Metab* 2011; 14: 724–738.
- Baburamani AA, Ek CJ, Walker DW, et al. Vulnerability of the developing brain to hypoxic-ischemic damage: contribution of the cerebral vasculature to injury and repair? *Front Physiol* 2012; 3: 424.
- Sahni PV, Zhang J, Sosunov S, et al. Krebs cycle metabolites and preferential succinate oxidation following neonatal hypoxic-ischemic brain injury in mice. *Pediatr Res* 2018; 83: 491–497.
- Chouchani ET, Pell VR, Gaude E, et al. Ischaemic accumulation of succinate controls reperfusion injury through mitochondrial ROS. *Nature* 2014; 515: 431–435.
- Wu TW, Tamrazi B, Hsu KH, et al. Cerebral lactate concentration in neonatal hypoxic-ischemic encephalopathy: in relation to time, characteristic of injury, and serum lactate concentration. *Front Neurol* 2018; 9: 293.
- Cherif H, Duhamel F, Cecyre B, et al. Receptors of intermediates of carbohydrate metabolism, GPR91 and GPR99, mediate axon growth. *PLoS Biol* 2018; 16: e2003619.
- Liu C, Wu J, Zhu J, et al. Lactate inhibits lipolysis in fat cells through activation of an orphan G-protein-coupled receptor, GPR81. *J Biol Chem* 2009; 284: 2811–2822.
- Hamel D, Sanchez M, Duhamel F, et al. G-protein-coupled receptor 91 and succinate are key contributors in neonatal postcerebral hypoxia-ischemia recovery. *Arterioscler Thromb Vasc Biol* 2014; 34: 285–293.
- Lee YJ, Shin KJ, Park SA, et al. G-protein-coupled receptor 81 promotes a malignant phenotype in breast cancer through angiogenic factor secretion. *Oncotarget* 2016; 7: 70898–70911.
- Brown TP and Ganapathy V. Lactate/GPR81 signaling and proton motive force in cancer: role in angiogenesis, immune escape, nutrition, and Warburg phenomenon. *Pharmacol Ther* 2020; 206: 107451.
- Hoque R, Farooq A, Ghani A, et al. Lactate reduces liver and pancreatic injury in toll-like receptor- and inflammasome-mediated inflammation via GPR81-mediated suppression of innate immunity. *Gastroenterology* 2014; 146: 1763–1774.
- Madaan A, Chaudhari P, Nadeau-Vallee M, et al. Cell-localized G-protein-coupled receptor 81 (hydroxycarboxylic acid receptor 1) regulates inner retinal vasculature via Norrin/WNT pathways. *Am J Pathol* 2019; 189: 1878–1896.
- Bergersen LH and Gjedde A. Is lactate a volume transmitter of metabolic states of the brain? *Front Neuroenergetics* 2012; 4: 5.
- Alvarez Z, Hyrossova P, Perales JC, et al. Neuronal progenitor maintenance requires lactate metabolism and PEPCCK-M-directed cataplerosis. *Cereb Cortex* 2016; 26: 1046–1058.
- Berthet C, Lei H, Thevenet J, et al. Neuroprotective role of lactate after cerebral ischemia. *J Cereb Blood Flow Metab* 2009; 29: 1780–1789.
- Shen Z, Jiang L, Yuan Y, et al. Inhibition of G protein-coupled receptor 81 (GPR81) protects against ischemic brain injury. *CNS Neurosci Ther* 2015; 21: 271–279.
- Rahman M, Muhammad S, Khan MA, et al. The beta-hydroxybutyrate receptor HCA2 activates a neuroprotective subset of macrophages. *Nat Commun* 2014; 5: 3944.
- Madaan A, Nadeau-Vallee M, Rivera JC, et al. Lactate produced during labor modulates uterine inflammation via GPR81 (HCA1). *Am J Obstet Gynecol* 2017; 216: 60 e61–60 e17.
- Percie Du Sert N, Hurst V, Ahluwalia A, et al. The ARRIVE guidelines 2.0: updated guidelines for reporting animal research. *J Cereb Blood Flow Metab* 2020; 40: 1769–1777.
- Gage GJ, Kipke DR and Shain W. Whole animal perfusion fixation for rodents. *J Vis Exp* 2012; 65: e3564.

30. Wang JW, Liu JY, Yan PH, et al. Effects of lactate on cell injury in primary cultures of rat cortical neurons during hypoxia/reoxygenation. *Zhongguo Ying Yong Sheng Li Xue Za Zhi* 2008; 24: 434–438.
31. Reed MJ, Karres N, Eyman D, et al. Culture of murine aortic explants in 3-dimensional extracellular matrix: a novel, miniaturized assay of angiogenesis in vitro. *Microvasc Res* 2007; 73: 248–252.
32. Vannucci RC and Vannucci SJ. A model of perinatal hypoxic-ischemic brain damage. *Ann N Y Acad Sci* 1997; 835: 234–249.
33. Sirinyan M, Sennlaub F, Dorfman A, et al. Hyperoxic exposure leads to nitrative stress and ensuing microvascular degeneration and diminished brain mass and function in the immature subject. *Stroke* 2006; 37: 2807–2815.
34. Benedek A, Moricz K, Juranyi Z, et al. Use of TTC staining for the evaluation of tissue injury in the early phases of reperfusion after focal cerebral ischemia in rats. *Brain Res* 2006; 1116: 159–165.
35. Bederson JB, Pitts LH, Germano SM, et al. Evaluation of 2,3,5-triphenyltetrazolium chloride as a stain for detection and quantification of experimental cerebral infarction in rats. *Stroke* 1986; 17: 1304–1308.
36. Badea A, Ali-Sharief AA and Johnson GA. Morphometric analysis of the C57BL/6J mouse brain. *Neuroimage* 2007; 37: 683–693.
37. Zhang Y, Chen K, Sloan SA, et al. An RNA-sequencing transcriptome and splicing database of glia, neurons, and vascular cells of the cerebral cortex. *J Neurosci* 2014; 34: 11929–11947.
38. Sitaras N, Rivera JC, Noueihed B, et al. Retinal neurons curb inflammation and enhance revascularization in ischemic retinopathies via proteinase-activated receptor-2. *Am J Pathol* 2015; 185: 581–595.
39. Sapieha P, Sirinyan M, Hamel D, et al. The succinate receptor GPR91 in neurons has a major role in retinal angiogenesis. *Nat Med* 2008; 14: 1067–1076.
40. Pearce WJ. Fetal cerebrovascular maturation: effects of hypoxia. *Semin Pediatr Neurol* 2018; 28: 17–28.
41. Nalivaeva NN, Turner AJ and Zhuravin IA. Role of prenatal hypoxia in brain development, cognitive functions, and neurodegeneration. *Front Neurosci* 2018; 12: 825.
42. Luo J, Martinez J, Yin X, et al. Hypoxia induces angiogenic factors in brain microvascular endothelial cells. *Microvasc Res* 2012; 83: 138–145.
43. Yin KJ, Hamblin M and Chen YE. Angiogenesis-regulating microRNAs and ischemic stroke. *Curr Vasc Pharmacol* 2015; 13: 352–365.
44. Bramlett HM and Dietrich WD. Pathophysiology of cerebral ischemia and brain trauma: similarities and differences. *J Cereb Blood Flow Metab* 2004; 24: 133–150.
45. Chu HX and Jones NM. Changes in hypoxia-inducible factor-1 (HIF-1) and regulatory prolyl hydroxylase (PHD) enzymes following hypoxic-ischemic injury in the neonatal rat. *Neurochem Res* 2016; 41: 515–522.
46. Thorpe RB, Hubbell MC, Silpanisong J, et al. Chronic hypoxia attenuates the vasodilator efficacy of protein kinase G in fetal and adult ovine cerebral arteries. *Am J Physiol Heart Circ Physiol* 2017; 313: H207–H219.
47. Wang Q, Hu Y, Wan J, et al. Lactate: a novel signaling molecule in synaptic plasticity and drug addiction. *Bioessays* 2019; 41: e1900008.
48. Margineanu MB, Mahmood H, Fiumelli H, et al. L-lactate regulates the expression of synaptic plasticity and neuroprotection genes in cortical neurons: a transcriptome analysis. *Front Mol Neurosci* 2018; 11: 375.
49. Husain Z, Huang Y, Seth P, et al. Tumor-derived lactate modifies antitumor immune response: effect on myeloid-derived suppressor cells and NK cells. *J Immunol* 2013; 191: 1486–1495.
50. Hunt TK, Aslam R, Hussain Z, et al. Lactate, with oxygen, incites angiogenesis. *Adv Exp Med Biol* 2008; 614: 73–80.
51. Ruan GX and Kazlauskas A. Lactate engages receptor tyrosine kinases axl, Tie2, and vascular endothelial growth factor receptor 2 to activate phosphoinositide 3-kinase/akt and promote angiogenesis. *J Biol Chem* 2013; 288: 21161–21172.
52. Husted AS, Trauelsen M, Rudenko O, et al. GPCR-Mediated signaling of metabolites. *Cell Metab* 2017; 25: 777–796.
53. Ahmed K. Biological roles and therapeutic potential of hydroxy-carboxylic acid receptors. *Front Endocrinol (Lausanne)* 2011; 2: 51.
54. Hu J, Cai M, Liu Y, et al. The roles of GRP81 as a metabolic sensor and inflammatory mediator. *J Cell Physiol* 2020; 235: 8938–8950.
55. Ahmed K, Tunaru S, Tang C, et al. An autocrine lactate loop mediates insulin-dependent inhibition of lipolysis through GPR81. *Cell Metab* 2010; 11: 311–319.
56. Berg KA and Clarke WP. Making sense of pharmacology: Inverse agonism and functional selectivity. *Int J Neuropsychopharmacol* 2018; 21: 962–977.
57. Alessandri B, Schwandt E, Kamada Y, et al. The neuroprotective effect of lactate is not due to improved glutamate uptake after controlled cortical impact in rats. *J Neurotrauma* 2012; 29: 2181–2191.
58. Horn T and Klein J. Neuroprotective effects of lactate in brain ischemia: dependence on anesthetic drugs. *Neurochem Int* 2013; 62: 251–257.
59. Ogunshola OO, Stewart WB, Mihalcik V, et al. Neuronal VEGF expression correlates with angiogenesis in postnatal developing rat brain. *Brain Res Dev Brain Res* 2000; 119: 139–153.
60. Isenberg JS, Annis DS, Pendrak ML, et al. Differential interactions of thrombospondin-1, -2, and -4 with CD47 and effects on cGMP signaling and ischemic injury responses. *J Biol Chem* 2009; 284: 1116–1125.
61. Morland C, Lauritzen KH, Puchades M, et al. The lactate receptor, G-protein-coupled receptor 81/hydroxycarboxylic acid receptor 1: expression and action in brain. *J Neurosci Res* 2015; 93: 1045–1055.
62. Morland C, Andersson KA, Haugen OP, et al. Exercise induces cerebral VEGF and angiogenesis via the lactate receptor HCAR1. *Nat Commun* 2017; 8: 15557.

63. Masaoka H, Klatzo I, Tomida S, et al. Role of circulatory disturbances in the development of post-ischemic brain edema. *Neurochem Pathol* 1988; 9: 21–29.
64. Bornstein P. Thrombospondins function as regulators of angiogenesis. *J Cell Commun Signal* 2009; 3: 189–200.
65. Christopherson KS, Ullian EM, Stokes CC, et al. Thrombospondins are astrocyte-secreted proteins that promote CNS synaptogenesis. *Cell* 2005; 120: 421–433.
66. Lu Z and Kipnis J. Thrombospondin 1 – a key astrocyte-derived neurogenic factor. *Faseb J* 2010; 24: 1925–1934.
67. Chu LY, Ramakrishnan DP and Silverstein RL. Thrombospondin-1 modulates VEGF signaling via CD36 by recruiting SHP-1 to VEGFR2 complex in microvascular endothelial cells. *Blood* 2013; 122: 1822–1832.
68. Maxhimer JB, Shih HB, Isenberg JS, et al. Thrombospondin-1/CD47 blockade following ischemia-reperfusion injury is tissue protective. *Plast Reconstr Surg* 2009; 124: 1880–1889.
69. Rohrs JA, Sulistio CD and Finley SD. Predictive model of thrombospondin-1 and vascular endothelial growth factor in breast tumor tissue. *NPJ Syst Biol Appl* 2016; 2
70. Risher WC and Eroglu C. Thrombospondins as key regulators of synaptogenesis in the Central nervous system. *Matrix Biol* 2012; 31: 170–177.
71. Patel R and Dickenson AH. Mechanisms of the gabapentinoids and alpha 2 Delta-1 calcium channel subunit in neuropathic pain. *Pharmacol Res Perspect* 2016; 4: e00205.
72. Eroglu C, Allen NJ, Susman MW, et al. Gabapentin receptor alpha2delta-1 is a neuronal thrombospondin receptor responsible for excitatory CNS synaptogenesis. *Cell* 2009; 139: 380–392.
73. Jaffer H, Morris VB, Stewart D, et al. Advances in stroke therapy. *Drug Deliv Transl Res* 2011; 1: 409–419.